Supporting Information

N-doping of graphene oxide at low temperature for oxygen reduction reaction

Hengcong Tao,[a] Chao Yan,[b] Alex W. Robertson,[c] Yunnan Gao,[a] Jingjing Ding,[a] Yuqin Zhang,[a] Tao Ma,[a] and Zhenyu Sun[a]*

[a] *State Key Laboratory of Organic-Inorganic Composites, Beijing University of Chemical Technology, Beijing 100029, China. Corresponding email: sunzy@mail.buct.edu.cn*

[b] *School of Material Science & Engineering, Jiangsu University of Science and Technology, Zhenjiang 212003, China*

[c] *Department of Materials, University of Oxford, Oxford, OX1 3PH, United Kingdom*

Experimental

All chemicals used in this work were of analytical grade and used as supplied. Graphene oxide powder (purity > 98.5 wt%) was purchased from Sinocarbon Graphene Marketing Center. Aqueous solution of ammonia (product number: A112083) was bought from Aladdin and used as received without purification. Acetone was acquired from Beijing Chemical Works (product number: B0701001).

N-doping of graphene oxide

Typically, 30 mg of graphene oxide powder was added into 10 mL of aqueous ammonia. The resulting dispersion was subjected to bath ultrasonication (KQ5200DE, 40 kHz) at certain temperature for 3 h. To keep the temperature at fixed values, we utilized ice and circulating water. The precipitate was isolated by ultracentrifugation (TGL-16A) and washed with deionized water and acetone three times, and then dried at 45 °C overnight.

Characterization

X-ray powder diffraction (XRD) was performed with a D/MAX−RC diffractometer operated at 30 kV and 100 mA with Cu Kα radiation. Scanning electron microscopy

(SEM) was carried out using a field emission microscope (FEI Quanta 600 FEG) operated at 20 kV and equipped with an energy-dispersive X-ray spectrometer (EDX). Transmission electron microscopy (TEM) was conducted using an aberration corrected transmission electron microscope (JEOL 2200) with 80 kV accelerating voltage. TEM samples were prepared by depositing a droplet of suspension onto a Cu grid coated with a lacey carbon film. Atomic force microscopy (AFM) images were obtained on a 5500 AFM/SPM system (Agilent Technologies Inc., USA) in tapping mode at room temperature. UV-vis absorption spectroscopy was conducted using a PERSEE spectrophotometer. X-ray photoelectron spectra (XPS) were carried out on a K-Alpha spectrometer (Thermo Fisher Scientific Inc., Switzerland) equipped with a monochromatic Al Kα source operated at 150 W. Nitrogen adsorption/desorption measurements were made on a BELSORP-max (MicrotracBEL) analyzer to determine the Brunauer-Emmett-Teller (BET) surface area. The samples were degassed in vacuum at 200 ºC for 8 h prior to N_2 adsorption at - 195 ºC. Raman spectra of NGO and GO films were collected with a Renishaw in Via Raman microscope with a He/Ne Laser excitation at 532 nm.

Electrochemical measurement

Cyclic voltammetry (CV) and linear-scan voltammetry (LSV) were carried out in a three-electrode system using Ag/AgCl as reference electrode, Pt wire as counter electrode and glassy carbon as working electrode on a CHI 760E potentiostat (CHI Inc., USA). Rotating disk electrode (RDE) experiments were run on a AFMSRCE RDE control system (Pine Inc., USA). In all of the electrochemical measurements, 0.1 M KOH aqueous solution saturated with O_2 was used as the electrolyte.

The number of electrons transferred per oxygen molecule on electrodes, n, was estimated by RDE voltammetry using the Koutecky-Levich (K-L) equation:

$$\frac{1}{j} = \frac{1}{j_k} + \frac{1}{j_L} = \frac{1}{j_k} + \frac{1}{B\sqrt{\omega}}$$

where $B = 0.62nFAD^{2/3}\nu^{-1/6}C^*$, j, j_L and j_K are the measured current density, diffusion-limiting current density and kinetic-limiting current density at a specific potential, respectively; n, the number of electrons transferred; D, the diffusion coefficient of the

analyte, in this case O_2 (1.9×10^{-5} cm^2 s^{-1}); F, the Faraday constant (96485 C mol^{-1}); A, the geometric area of the electrode (0.19625 cm^2); v, the kinematic viscosity of the electrolyte (0.01 cm^2 s^{-1}), and C^* the solubility of oxygen in the electrolyte, which for the case of KOH (0.1 M) was taken to be 1.2×10^{-6} mole cm^{-3}.[1]

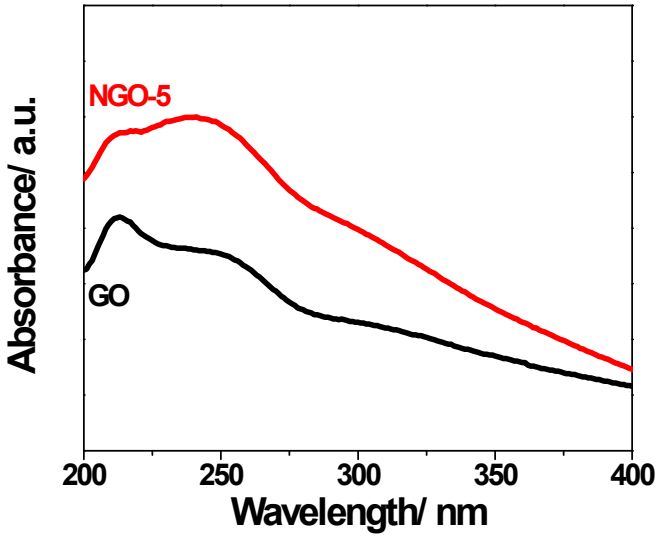

Fig. S1 Ultraviolet-visible spectra of GO and NGO-5 dispersions.

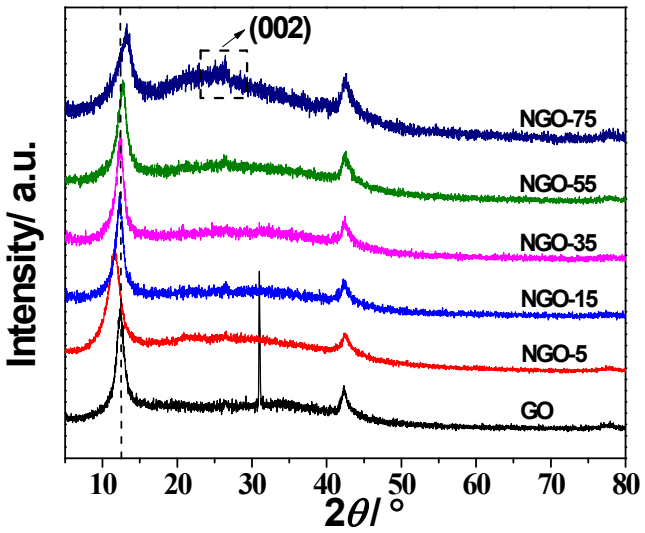

Fig. S2 XRD patterns of GO, and NGO samples obtained at varying ultrasonic bath temperatures.

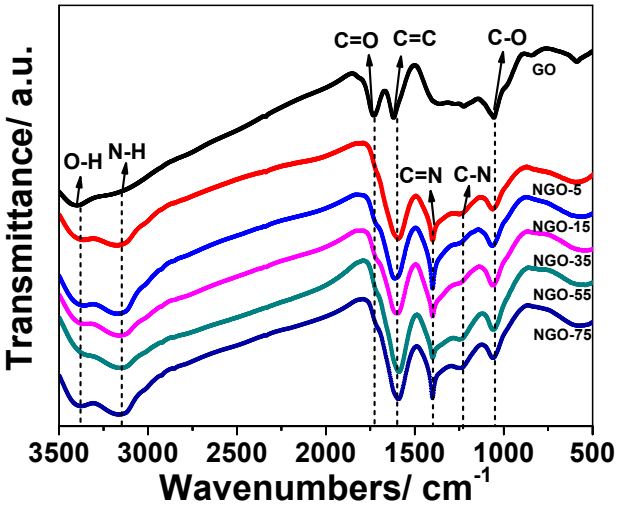

Fig. S3 FTIR spectra of GO and NGO samples.

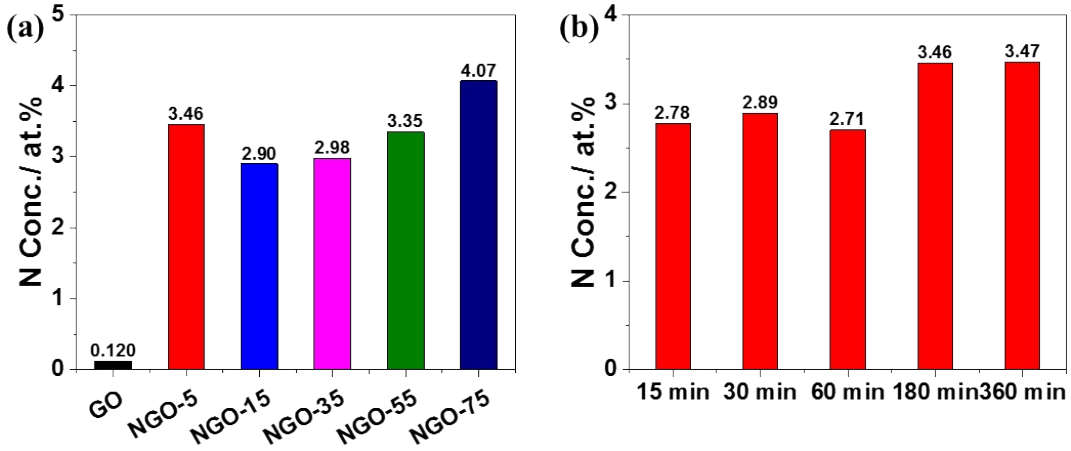

Fig. S4 Element analysis results: (a) The atomic content (at.%) of N in GO and NGO samples. (b) The atomic content (at.%) of N in NGO-5 versus ultrasonic time.

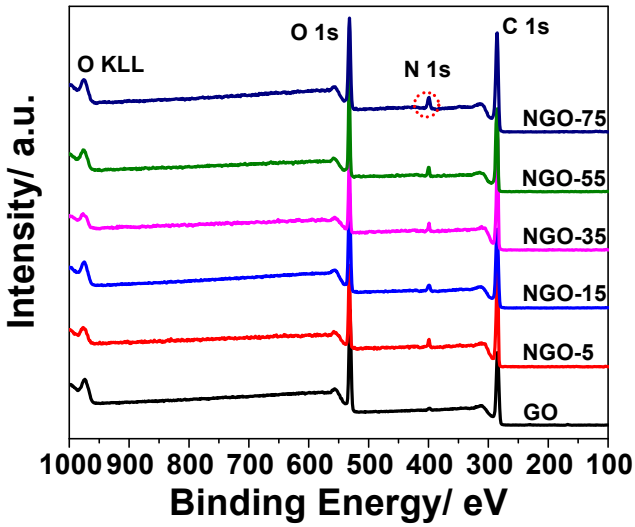

Fig. S5 Wide-survey XPS spectra of GO and NGO samples.

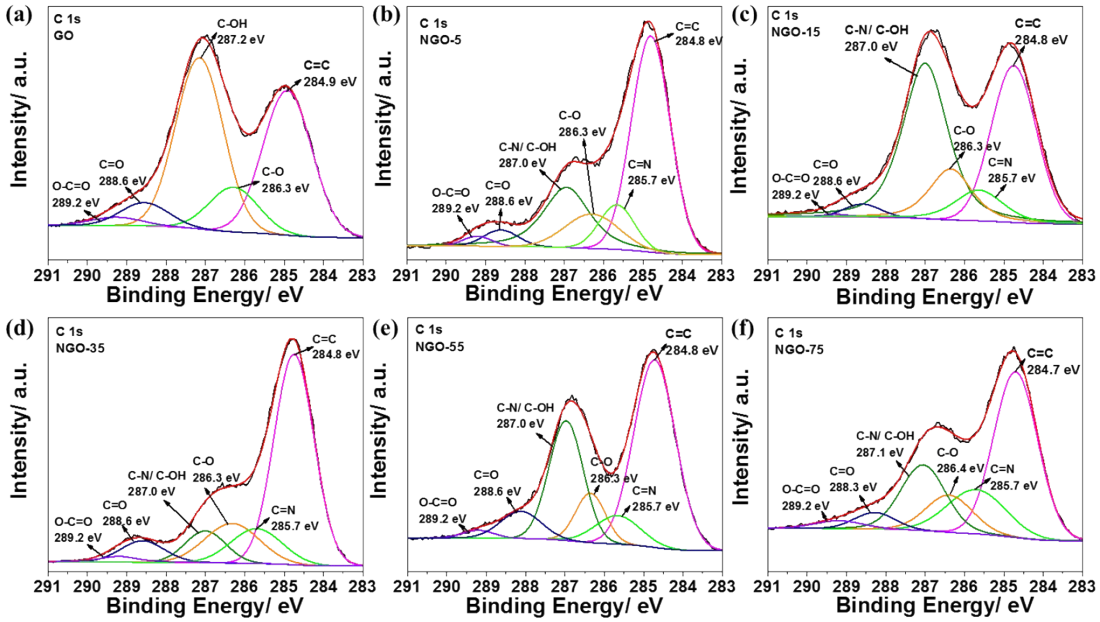

Fig. S6 C 1s XPS spectra of GO and NGO samples.

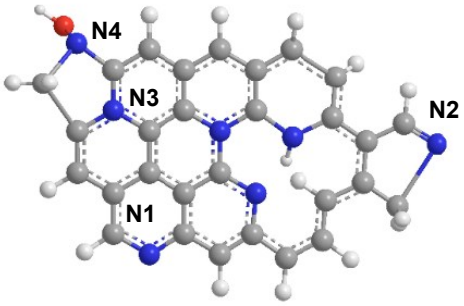

Fig. S7 Schematic of bonding configuration of N functionalities in NGO (N1: pyridinic N, N2: pyrrolic N, N3: quaternary N, N4: oxidic N).

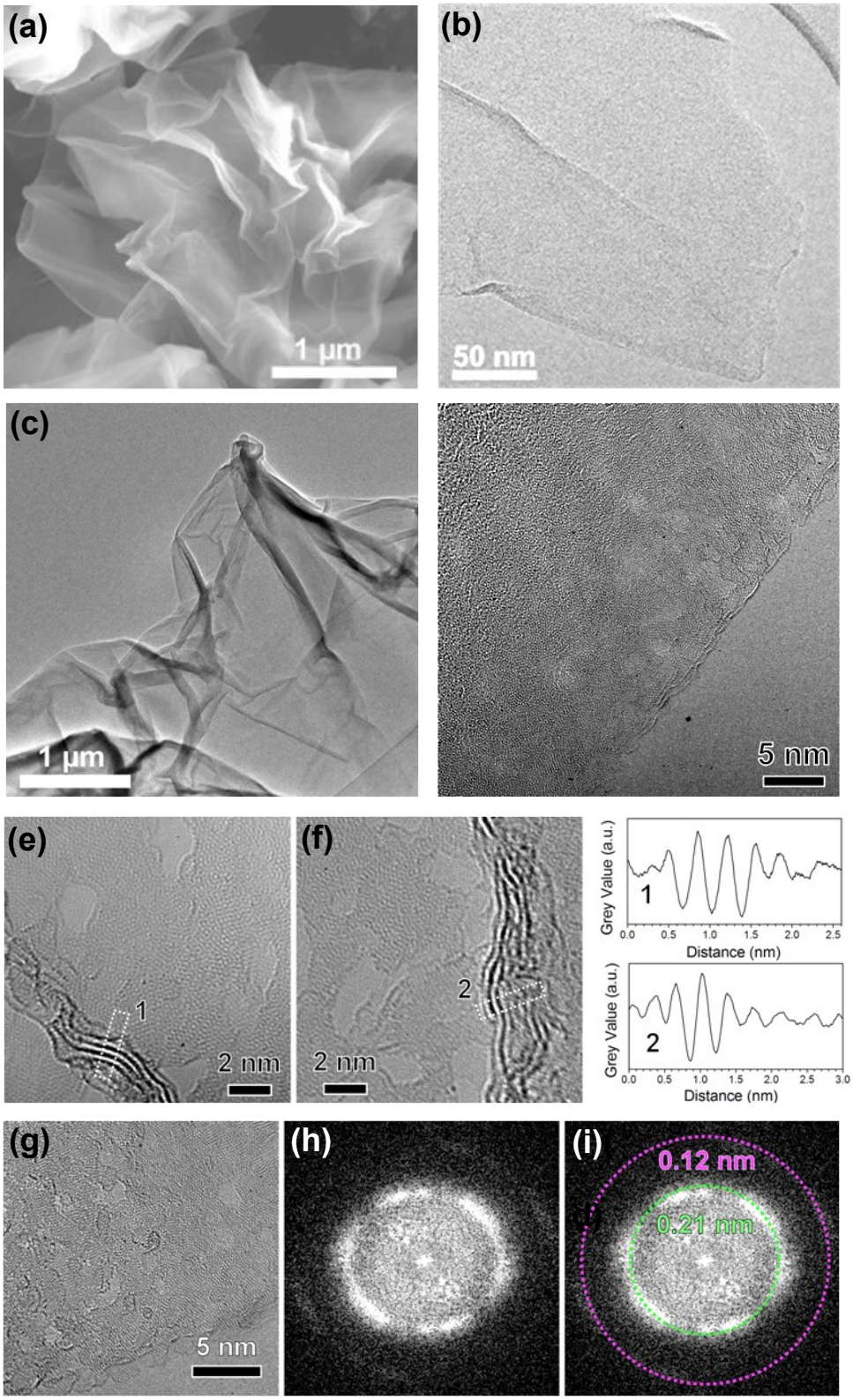

Fig. S8 (a) SEM and (b) TEM images of GO. (c) Low-magnification TEM image of NGO-5 flakes. (d)-(g) ACTEM images of a possible two-layer, four-layer, five-layer and monolayer NGO-5 sheet, respectively. (h) FFT image of g. (i) The FFT image marked by dash lines. The box averaged intensity profiles indicated along the rectangles

in e and f were taken to get the respective intensity profiles. From the Gaussian fits to the minima corresponding to the dark layer fringes, we can measure interlayer spacings by taking the difference of the x_c values of each peak. This gives values of 0.36 nm, 0.36 nm, and 0.37 nm.

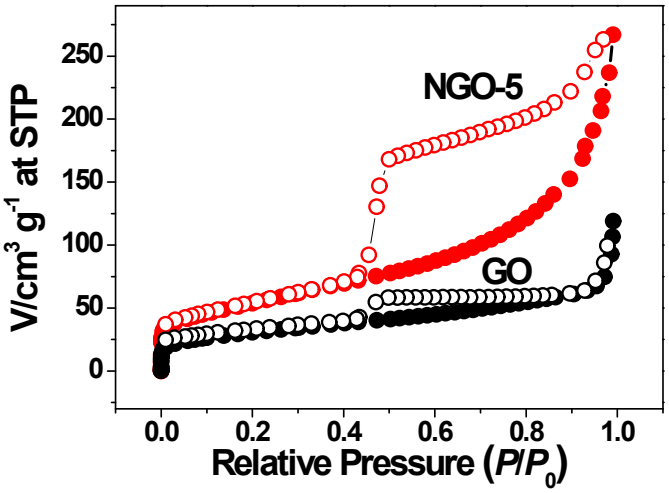

Fig. S9 N_2 adsorption/desorption isotherms of GO and NGO-5 which exhibit a Type IV isotherm based on the Brunauer, Deming, Deming and Teller (BDDT) classification in both cases.[2] A gradually increasing adsorption was observed in the relative pressure (P/P_0) range 0.2-0.4, indicative of mesoporous character. The small adsorption in the P/P_0 range 0.05 may arise from some microporosities, and the slowly increasing adsorption in the mid-range of P/P_0 was due to multilayer adsorption. Both GO and NGO-5 showed a Type H2 loop, being correlated with pores with narrow necks and wide bodies and network effects. The Brunauer-Emmett-Teller (BET) surface areas of GO and NGO-5 were determined as 106.2 and 188.2 $m^2 g^{-1}$, respectively.

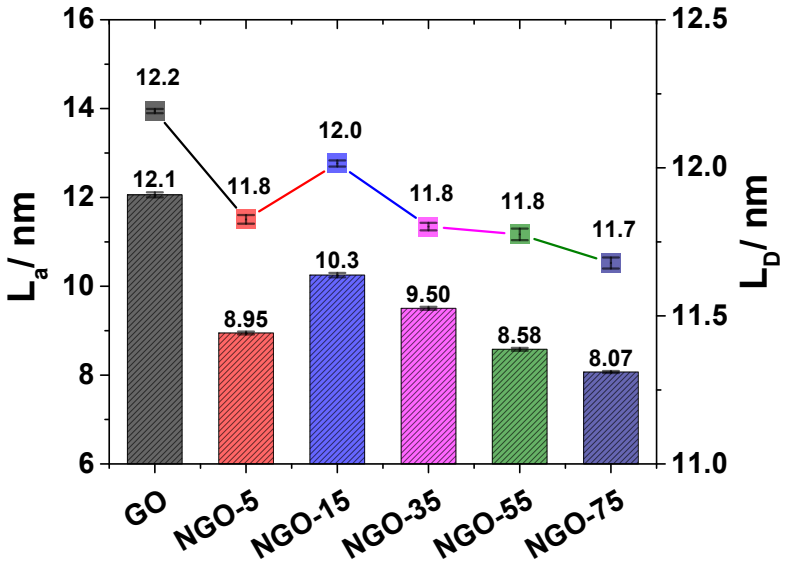

Fig. S10 The in-plane crystallite size, L_a, and the distance between defects, L_D, of GO and NGO samples.

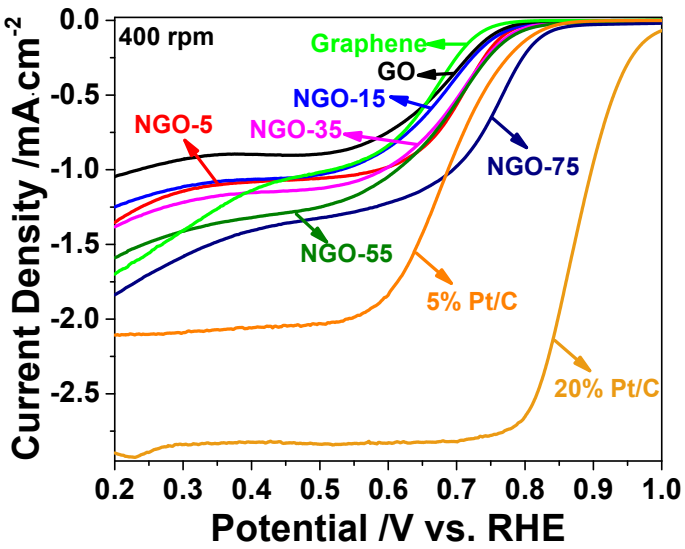

Fig. S11 Linear scan voltammogram curves of GO, liquid-exfoliated graphene, NGO samples, and commercial 5% and 20% Pt/C in O_2-saturated 0.1 M KOH at scan rates of 5 mV s^{-1}.

The voltammograms of NGO samples shown in Fig. S11 do not reach steady state. However, this is an inherent property of truly metal-free catalysts,[3] and is partly to concurrent direct and sequential reduction of oxygen, and due to structural inhomogeneity of the involved active sites, where the most active sites initially drive the ORR at less overpotential while the less active ones are triggered on at higher

overpotentials. This observation also attests to the fact that the reduction of oxygen on metal-free catalysts proceeds via hydrogen peroxide which is then further reduced to OH^-, while some of it undergoes disproportionation.

Table S1. Comparison of N contents, N configuration concentrations, current densities at 0. 5 V (vs. RHE) and onset potentials (vs. RHE) for GO, liquid-exfoliated graphene and NGO samples.

Sample	**Nitrogen Content (at.%)***	**Graphitic N Conc. (at.%)†**	**Pyridinic N Conc. (at.%)†**	**Pyrrolic N Conc. (at.%)†**	**Oxidic N Conc. (at.%)†**	**$\|j\|$ at 0.5 V (mA cm^{-2})‡**	**Onset Potential (V)**
GO	0.12	≈ 0	≈ 0	≈ 0	≈ 0	0.69	0.71
Graphene	0	0	0	0	0	1.01	0.66
NGO-5	3.46	0.55	0.36	2.44	0.10	1.07	0.79
NGO-15	2.90	0.46	0.28	2.03	0.12	1.02	0.78
NGO-35	2.98	0.45	0.26	2.2	0.08	1.13	0.81
NGO-55	3.35	0.56	0.81	1.85	0.14	1.29	0.82
NGO-75	4.07	0.62	1.00	2.29	0.16	1.32	0.84

*Nitrogen content determined by elemental analysis. †Nitrogen configuration concentration evaluated by XPS. ‡ORR current density obtained from current divided by geometric area of electrode surface (0.19625 cm^2).

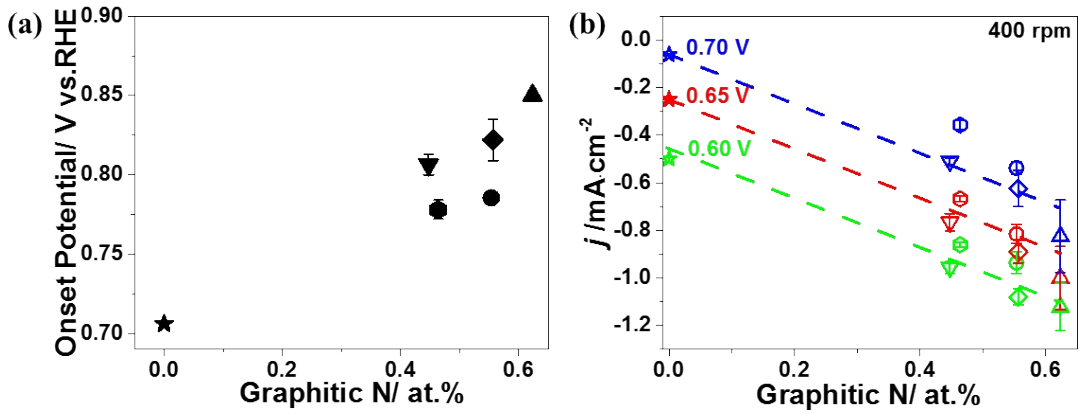

Fig. S12 (a) Correlation between current densities at 0.7, 0.65, 0.6 V (vs. RHE) with

graphitic N concentrations. (b) Correlation of onset potentials with graphitic N concentrations.

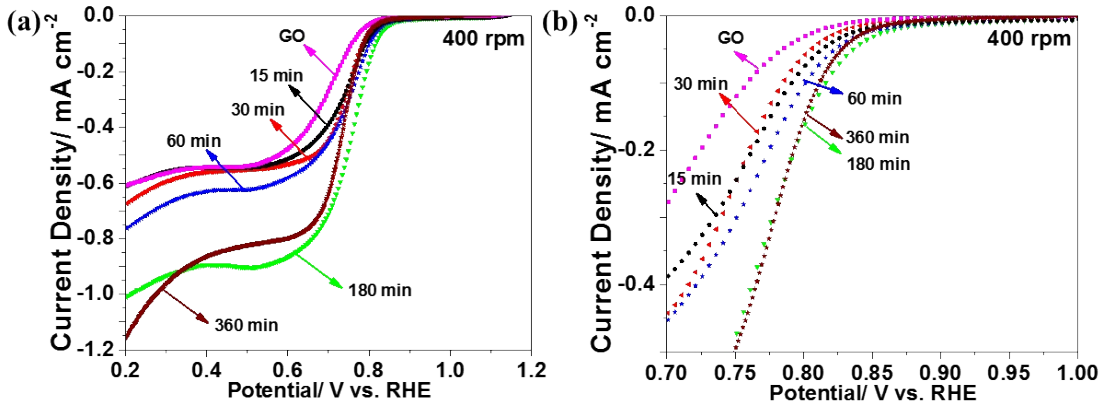

Fig. S13 LSVs of GO, NGO-5 produced at varying ultrasonic time in oxygen-saturated 0.1 M KOH at a scan rate of 5 mV s^{-1} in the potential range of (a) 0.2-1.2 V and (b) 0.7-1.0 V.

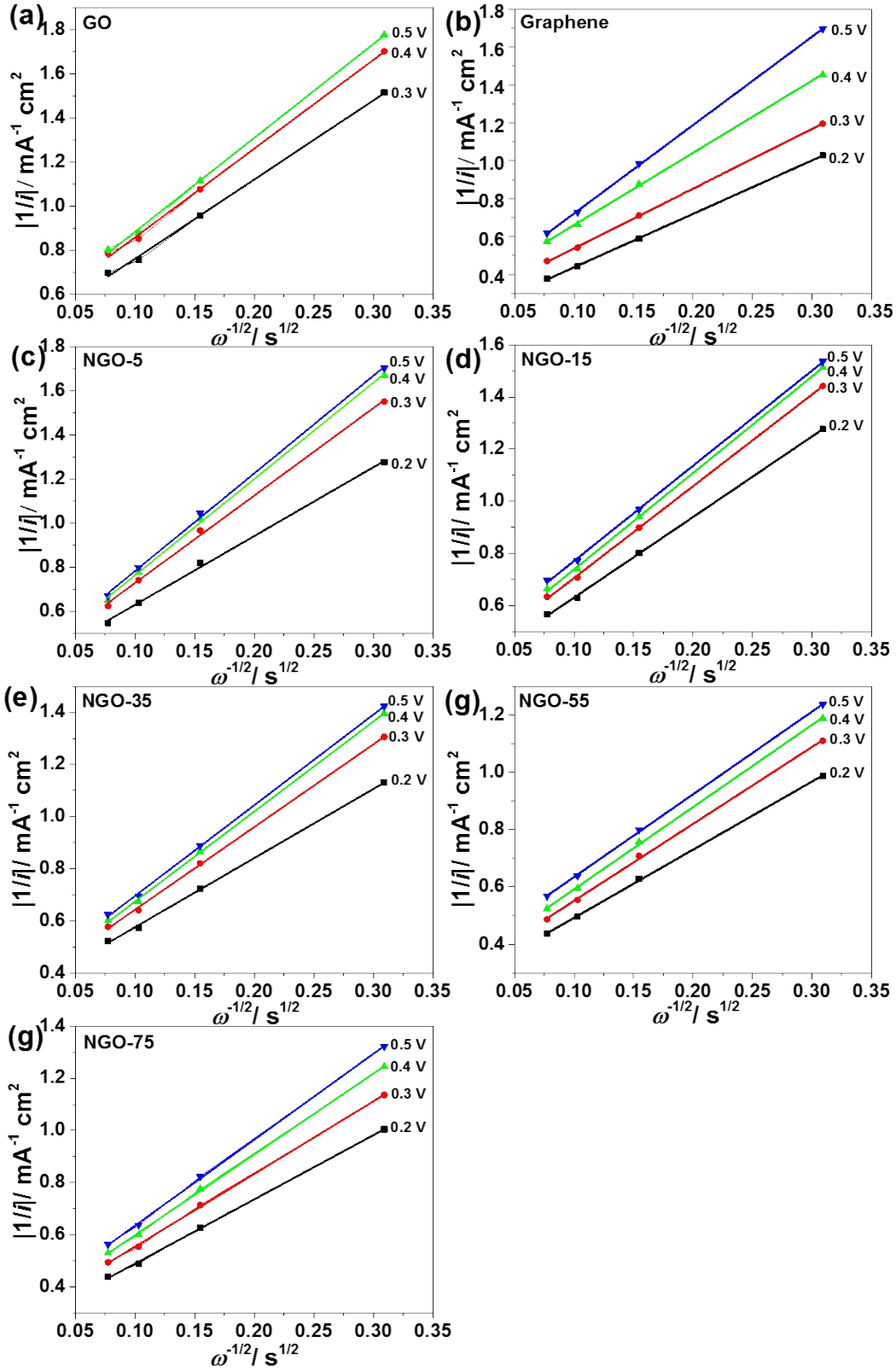

Fig. S14 Koutecky–Levich plots of (a) GO, (b) liquid-exfoliated graphene, (c) NGO-5, (d) NGO-15, (e) NGO-35, (f) NGO-55 and (g) NGO-75.

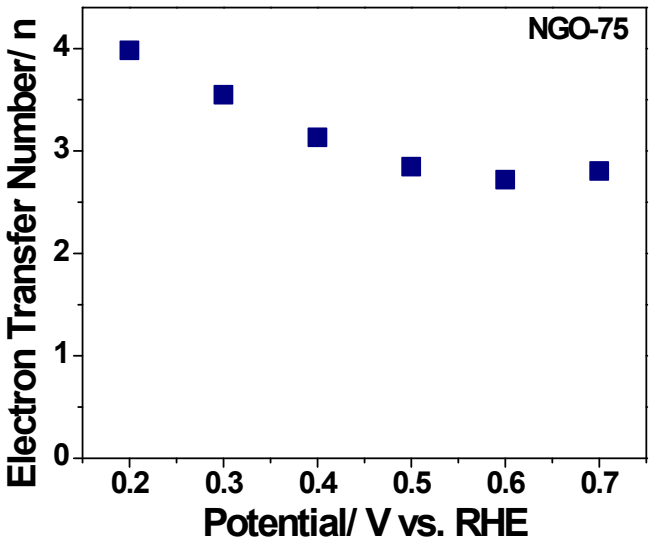

Fig. S15 Number of electrons transferred at different potentials for NGO-75.

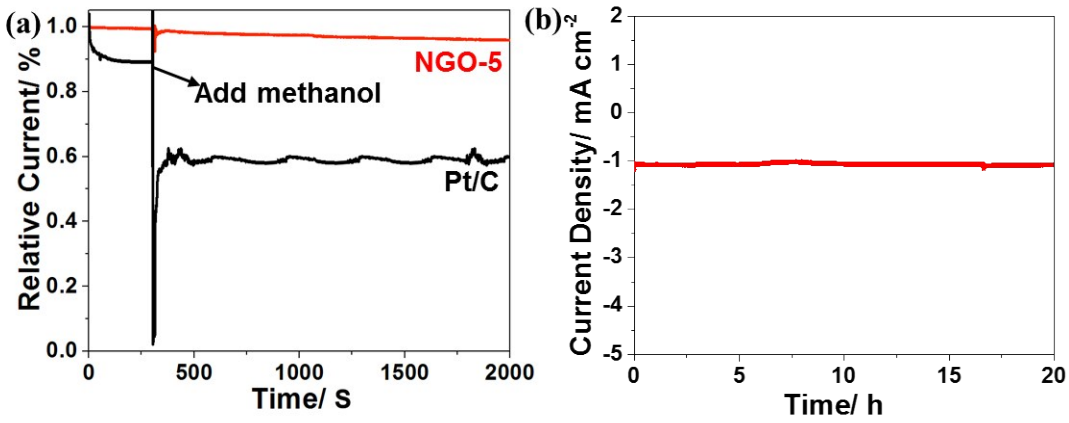

Fig. S16 (a) Chronoamperometric responses at 0.56 V (vs. RHE) in O_2-saturated 0.1 M KOH on NGO-5 and commercial 5% Pt/C electrodes (100 rpm) followed by introducing CH_3OH (3 M) at 300 s. (b) Durability evaluation of NGO-5 at a potential of 0.56 V (vs. RHE) in O_2-saturated 0.1 M KOH and at a rotation speed of 100 rpm for 20 h.

Reference

1 F. X. Ma, J. Wang, F. B. Wang and X. H. Xia, *Chem. Commun.*, 2015, 51, 1198–1201.

2 K. S. W. Sing, D. H. Everett, R. A. W. Haul, L. Moscou, R. A. Pierotti, J.

Rouquérol and T. Siemieniewska, *Pure Appl., Chem.,* 1985, 57, 603–619.

3 L. M. Dai, Y. H. Xue, L. T. Qu, H. J. Choi and J. B. Baek, *Chem. Rev.,* 2015, 115, 4823–4892.